RAA 2018 Vol. **18** No. **12**, 155(12pp) doi: 10.1088/1674–4527/18/12/155

http://www.raa-journal.org *http://iopscience.iop.org/raa*

Research in Astronomy and Astrophysics

Variable stars in M37

Ajaz Ahmad Dar[1,2,3], Padmakar Singh Parihar[3], Parvej Saleh[4] and Manzoor Ahmad Malik[1]

[1] Department of Physics, University of Kashmir, Hazratbal 190006 Srinagar-J&K, India; *mmalik@kashmiruniversity.ac.in*

[2] Department of Physics, Islamia College of Science and Commerce, Hawal, Srinagar-19002, J&K, India

[3] Indian Institute of Astrophysics, Koramagala-560034, Bangalore, India

[4] Applied Sciences Department, Gowhati, University of Assam, India

Received 2018 May 24; accepted 2018 July 18

Abstract The CCD photometric observations of open star cluster M37 (NGC 2099) were carried out up to a limiting magnitude of $V \sim 20$ in both B and V filters to search for variable stars using a 2k×4k CCD and the 1.3 m telescope at the Vainu Bapu Observatory, Kavalur. A total of 314 stars were in the first observing run, out of which 60 were identified as variables. Eight out of the identified 60 variables are classified as W UMa binary stars. For model fitting, we used PHOEBE based on the W-D code to estimate the physical parameters of these newly detected W UMa binaries that theoretically best match the observed light curves.

Key words: techniques: photometric — astronomical instrumentation — methods and techniques — astrometry and celestial mechanics — (stars:) binaries: eclipsing

1 INTRODUCTION

Star clusters, particularly open clusters, are the best laboratories to study stellar evolution as these clusters provide a wealth of information about stars like their age, distance, initial composition and range of masses. Star clusters can contain different classifications of variable stars, as stars show variability at different stages during their evolutionary phases (Lata et al. 2011). Some of the classes of variable stars found in open clusters are (i) pulsating variables, (ii) eclipsing contact and detached variables, (iii) rotating variables, (iv) Delta Scuti (δ Scuti) type variables, (v) eruptive variables, (vi) cataclysmic variables, etc. (Kang et al. 2007; Hargis et al. 2005). The rich Galactic open star cluster NGC 2099, commonly known as Messier 37 or M37, is located in the Galactic anti-center direction in Auriga ($\alpha_{2000} = 5^{\rm h}52^{\rm m}17.6^{\rm s}$, $\delta_{2000} = 32°33'40''$). M37 or NGC 2099 is an interesting object to search for new variable stars as it is a rich open cluster with nearly 4000 stars having mass larger than 0.3 solar masses. Also, the age of this cluster is 550 Myr, because of which many of the stars in the cluster are active enough to be detected as variable stars with amplitude greater than a few milli-magnitudes (Hartman et al. 2008). Physical parameters of variable stars in a cluster can be estimated by analyzing the clusters in terms of their age, chemical abundance, distance and reddening (Kang et al. 2007). Ensemble photometry of hundreds of stars, constant as well as variable, in a single CCD frame enables us to obtain accurate and effective time-series data.

Section 2 describes the observations and data reduction process. In Section 3, we explain the identification of variable stars, and their periods and astrometric calibrations. The coordinates of observed objects with the VizieR list of objects are matched in Section 4. In Section 5, we discuss eight W UMa stars with their photometric parameters. Finally, we summarize our results in Section 6.

2 OBSERVATIONS AND DATA REDUCTION

The observing run that monitored the M37 open cluster region was carried out in both B and V bands from 2017 November 05 to 11 at the Vainu Bappu Observatory,

Table 1 Observing log for First Observing Run of M37

Date	Object	Filter	Total Frames	Exposure time (s)	Seeing (arcsec)
05–11–2017	M37	B, V	31	600, 360	1.6–1.8
07–11–2017	M37	B, V	20	600, 360	1.6–1.8
08–11–2017	M37	B, V	15	600, 360	1.6–2.0
09–11–2017	M37	B, V	31	600, 360	1.6–1.8
10–11–2017	M37	B, V	27	600, 360	1.6–2.0
11–11–2017	M37	B, V	29	600, 360	1.6–1.8

Kavalur with the 1.3 m JCB telescope. The CCD used for monitoring this cluster had a pixel size of 2k×4k with a field of view of about 0.299 arcsec pixel^{-1}, read noise of about 4.2 electrons and gain 0.745 e ADU^{-1}. Seeing, which was estimated from the full width at half maximum of point like stars in the image, ranged between 1.6 and 1.8 arcsec pixel^{-1} on most of the allotted nights except a few nights where it varied between 1.6 and 2 arcsec pixel^{-1}. Bias and twilight flats were also taken along with the target field of open cluster M37. The observing log is presented in Table 1. Barring a few thin cirrus clouds and occasionally high background counts, the sky remained transparent. We have taken longer exposure times in the B and V filters. The frames showing poor sky, bad seeing and with condensation are rejected in the analysis.

Cleaning and pre-processing of the CCD frames were done by the Image Reduction Analysis Facility (IRAF), which included bias subtraction, flat fielding and cosmic ray removal. IRAF tasks used for this purpose were zerocombine, flatcombine, imarith, imstat and in crutil cosmicrays. After correction for bias, flat fielding and cosmic ray removal, we identified a large number of bright stars in our field. The observations were carried out only in B and V frames. However, on a very clear photometric night under good seeing conditions, we took a few I-band frames. Among those we choose one as the reference frame, because the I-band minimizes the effect of nebular background and interstellar extinction. It also maximizes the signal-to-noise (S/N) ratio of red faint stars. Another advantage is that the effect of seeing is least in the I-band and the effect of color dependent atmospheric extinction, which is tedious to correct, is also minimized (Parihar et al. 2009).

We converted the coordinates of stars determined from the reference frame by taking the image shift and rotation into account. The centers of tens of bright stars were obtained using DAOPHOT (Stetson 1987), which is best suited for doing crowded field photometry. After that, the DAOMATCH and DAOMASTER programs by Stetson were used to obtain a good transformation relation for the stellar positions between the reference frame and any other observed frame. Next, the transformation relation generated by DAOMASTER was used to generate an input coordinate file for all stars whose coordinates were already determined in the reference frame. This coordinate file was used as an input to aperture photometry carried out by the PHOT task using Stetson's DAOPHOT-II. The outputs of DAOPHOT(PHOT) are dumped into data files corresponding to respective night frames, which include all the scientific information like flux and magnitude with errors of all the marked stars. Then an ensemble of these stars with their fluxes was made. As averaging is a powerful tool to minimize the effect of systematic noise, the ensemble data provided us with the standard deviation of the respective stars, on the basis of which comparison stars are chosen, i.e. the lower the standard deviation, the lower the variability of the star during that period. This process was carried out by a few simple python codes. Identification and removal of variables from the ensemble were done using a few basic statistics calculated for the light curve of each star. Stars in the ensemble exhibiting large standard deviations were removed. Among the rejected stars were the crowded stars and stars with cosmic rays in their aperture. Stars in the ensemble identified as variables were also removed from the ensemble and this process was repeated iteratively, until all the selected stars in the ensemble were found to be non-variable. The same procedure was adopted in Dar et al. (2018a) and Dar et al. (2018b). For standardization, we used the criteria adopted in Wang et al. (2015), Kang et al. (2007) and Kiss et al. (2001). The instrumental magnitudes were converted to the standard system with secondary stars. We selected 20 unsaturated and isolated bright stars showing long term stability during the observations as the secondary standards by performing simple differential photometry. The stars chosen were non-variable cases that were not located at the edges of the CCD frame. Ensemble normalization of Gilliland & Brown (1988) was used to normalize instrumental magnitudes of our time series V frames. The instrumental magnitudes v were transformed to standard magnitudes V using the equation

$$V = v + e_1 + e_2(B - V) + e_3X + e_4Y \ . \tag{1}$$

Table 2 Variables Identified in M37

S.No	ID	α (hh: mm: ss)	δ (dd: mm: ss)	Periods from Scargle periodogram	Periods from Schuster periodogram	Amplitude Scargle	$\langle V \rangle$	$\langle B-V \rangle$
(1)	(2)	(3)	(4)	(5)	(6)	(7)	(8)	(9)
1	ID002	5:52:54.87	32:34:12.9	4.3622	4.1054	0.0064	11.07	0.003
2	ID003	5:52:54.80	32:32:12.6	0.4439	0.2315	0.0045	10.40	0.05
3	ID006	5:52:52.41	32:35:11.2	0.4490	0.4384	0.0080	10.05	–0.02
4	ID009	5:52:51.63	32:31:05.4	0.2241	0.2246	0.0093	8.93	–0.101
5	ID010	5:52:50.99	32:29:41.9	0.4515	0.4655	0.0087	10.74	–0.06
6	ID012	5:52:50.44	32:29:52.5	0.4506	4.1054	0.0083	10.78	0.12
7	ID019	5:52:45.85	32:31:07.9	0.2244	0.4068	0.0082	11.33	–0.01
8	ID021	5:52:45.27	32:33:39.3	0.2238	0.2224	0.0105	10.44	–0.07
9	ID022	5:52:44.31	32:30:44.2	4.7603	5.1600	0.0046	11.63	0.02
10	ID024	5:52:42.54	32:33:55.9	4.8394	0.4561	0.0043	11.71	0.11
11	ID025	5:52:42.39	32:34:21.7	4.9933	6.4514	0.0084	9.44	–0.158
12	ID033	5:52:40.59	32:32:16.1	0.2235	0.3996	0.0076	8.04	0.682
13	ID040	5:52:39.39	32:36:18.8	4.7200	4.1054	0.0065	8.91	–0.117
14	ID043	5:52:38.37	32:33:05.8	4.6826	4.1054	0.0099	11.30	0.03
15	ID063	5:52:33.32	32:34:58.3	0.4527	0.4655	0.0048	9.10	–0.082
16	ID064	5:52:33.29	32:37:01.5	0.4337	0.4300	0.0060	10.02	–0.049
17	ID069	5:52:32.43	32:32:13.1	5.0064	5.1600	0.0093	10.43	–0.18
18	ID075	5:52:32.23	32:36:02.3	4.7836	5.0177	0.0080	11.68	0.14
19	ID097	5:52:20.45	32:35:04.2	4.9775	15.0533	0.0099	8.23	–0.094
20	ID102	5:52:18.93	32:32:17.9	0.4528	0.4655	0.0043	9.26	0.357
21	ID105	5:52:17.50	32:31:23.4	0.4522	6.4514	0.0053	10.61	–0.34
22	ID144	5:52:09.13	32:32:39.3	4.9886	5.1600	0.0148	9.23	0.323
23	ID146	5:52:08.61	32:32:15.4	4.8712	9.0320	0.0126	11.96	–0.19
24	ID153	5:52:07.01	32:31:19.2	4.8971	6.4514	0.0113	11.41	–0.11
25	ID155	5:52:06.71	32:31:10.2	4.7876	6.4514	0.0225	12.19	–0.3
26	ID158	5:52:06.46	32:34:47.4	4.7545	0.5575	0.0114	11.63	–0.09
27	ID160	5:52:06.22	32:31:57.8	4.7591	6.4514	0.0052	10.99	–0.39
28	ID162	5:52:05.72	32:33:18.8	4.7960	6.4514	0.0143	11.97	0.28
29	ID171	5:52:02.65	32:32:59.7	5.0238	5.1600	0.0077	11.82	–2.464
30	ID173	5:52:02.49	32:36:30.6	4.8927	5.1600	0.0076	9.25	–0.23
31	ID181	5:52:01.03	32:31:43.1	3.6518	0.4384	0.0137	8.86	–0.359
32	ID183	5:52:00.39	32:31:59.3	5.0364	5.1600	0.0075	10.82	–0.26
33	ID189	5:51:58.82	32:36:34.4	0.2362	0.4300	0.0043	10.86	–0.07
34	ID204	5:51:53.83	32:35:43.4	0.4495	5.1600	0.0059	11.65	–0.1
35	ID207	5:51:53.01	32:31:55.9	0.2235	1.9634	0.0052	12.11	0.04
36	ID212	5:51:50.89	32:31:51.2	4.8482	0.5575	0.0029	8.58	0.374
37	ID213	5:51:50.79	32:33:15.2	4.7707	5.0533	0.0055	11.63	0.03
38	ID215	5:51:50.67	32:32:17.4	0.4518	0.4655	0.0097	11.71	–0.07
39	ID227	5:51:46.87	32:37:05.1	0.4476	5.0177	0.0087	10.75	0.05
40	ID230	5:51:46.80	32:35:36.4	0.4503	0.4561	0.0068	10.04	–0.03
41	ID233	5:51:45.48	32:29:53.5	0.4505	0.4561	0.0071	11.84	0.01
42	ID239	5:51:45.00	32:30:41.8	0.4492	6.4514	0.0071	10.63	–0.23
43	ID240	5:51:44.74	32:32:20.3	0.4502	9.0320	0.0059	12.22	0.07
44	ID242	5:51:44.42	32:30:04.9	0.2233	1.9634	0.0064	11.09	–0.14
45	ID243	5:51:43.43	32:35:16.0	0.4376	0.4220	0.0059	10.82	0.61
46	ID245	5:51:43.09	32:32:39.1	0.4479	0.4384	0.0113	9.08	0.539
47	ID250	5:51:40.52	32:35:34.5	0.4474	0.4655	0.0096	11.24	0.05
48	ID253	5:51:39.59	32:35:54.7	0.4470	0.4384	0.0131	10.83	0.16
49	ID254	5:51:37.89	32:31:45.8	0.4445	0.4384	0.0092	12.52	–0.09
50	ID255	5:51:37.43	32:31:54.6	4.1198	0.5716	0.0037	11.75	–0.06
51	ID257	5:52:58.65	32:34:31.2	4.5326	0.4471	0.0179	11.00	0.35
52	ID260	5:52:58.92	32:36:32.3	0.4501	0.4471	0.0068	10.38	0.28
53	ID261	5:52:56.44	32:37:03.9	0.4510	0.4561	0.0122	9.07	0.165
54	ID263	5:52:53.67	32:37:42.5	0.2221	0.1530	0.0049	10.62	–9.82
55	ID268	5:52:28.98	32:31:52.9	0.4510	0.4561	0.0122	10.72	–0.18
56	ID269	5:52:26.72	32:33:11.2	0.4488	0.4384	0.0041	10.46	–0.23
57	ID275	5:52:20.93	32:30:56.9	5.0330	5.1600	0.0093	10.49	–0.3
58	ID299	5:52:17.58	32:30:35.2	0.4498	0.4561	0.0088	11.64	–0.17
59	ID300	5:52:17.26	32:32:56.8	0.4483	0.4561	0.0075	8.95	0.326
60	ID303	5:51:36.00	32:29:13.3	0.2235	5.1600	0.0098	9.80	–0.25

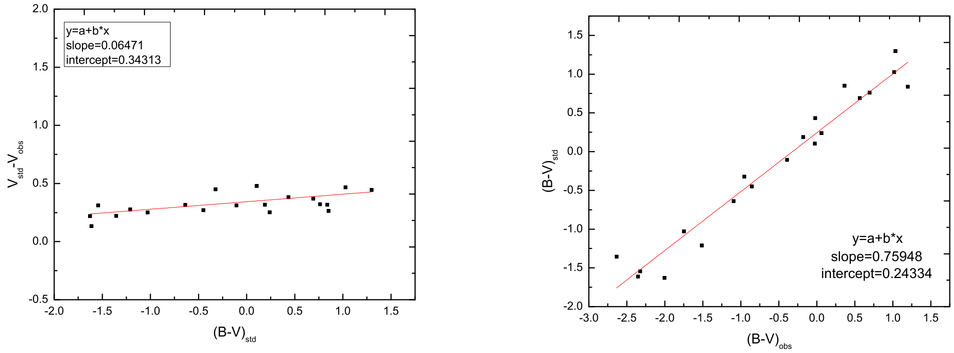

(a) (b)

Fig. 1 Fitting obtained by plotting $(B-V)_{\rm s}$ vs. $V_s - V_{\rm o}$ and $(B-V)_{\rm o}$ vs. $(B-V)_{\rm s}$.

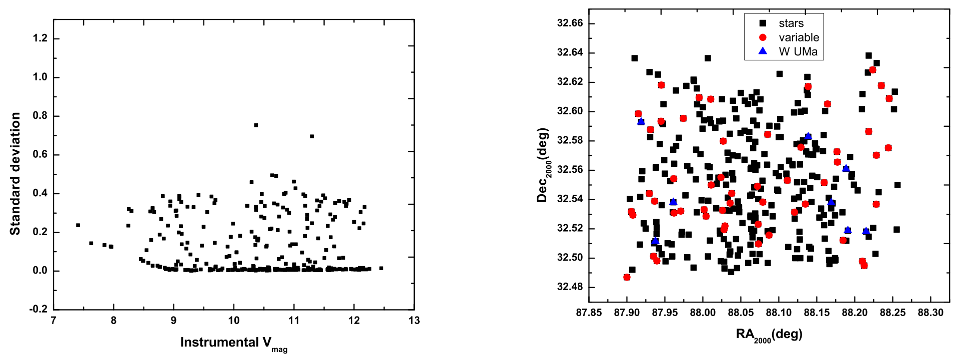

(a) (b)

Fig. 2 (a) Standard deviation vs. mean instrumental magnitude. (b) Plot between RA and Dec (in degrees) showing stars (■) selected from the M37 field frame, variables (●) and W UMa systems (▲).

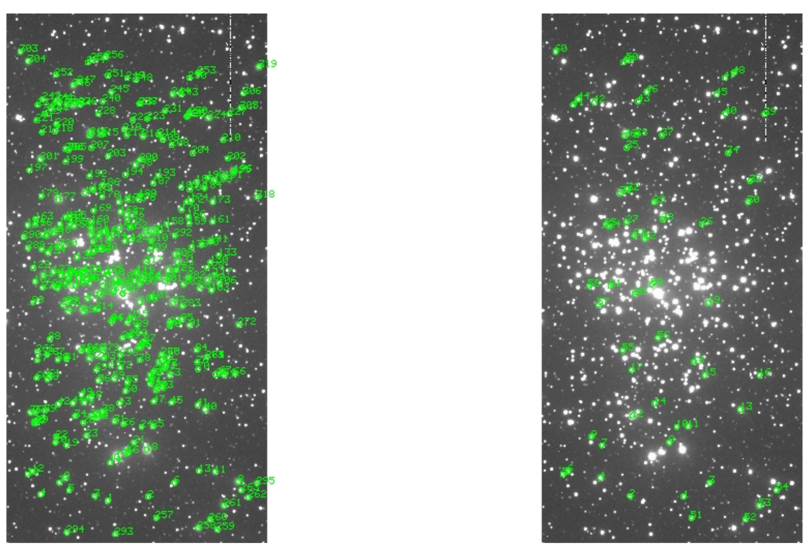

(a) (b)

Fig. 3 (a) All selected objects in the frame used in the analysis. (b) Sixty variables including eight W UMa stars are marked in the M37 field with their identification numbers as listed in Table 2.

For the B-frames, we used the equation

$$B = b + c_1 + c_2(B - V) + c_3X + c_4Y \ , \quad (2)$$

where B, V are standard magnitudes, b, v are instrumental magnitudes of images and X, Y are the position coordinates of a star in a CCD frame. The coefficients e_1, e_2, e_3 and e_4 appearing in Equation (1) and the coefficients c_1, c_2, c_3 and c_4 appearing in Equation (2) were calculated for CCD frames.

Figure 1 shows the best fit obtained between $(B - V)_{\mathrm{std}}$ vs. $V_{\mathrm{std}} - V_{\mathrm{obs}}$ and $(B - V)_{\mathrm{obs}}$ vs. $(B - V)_{\mathrm{std}}$.

3 IDENTIFICATION OF VARIABLES

All the light curves were visually inspected for the presence of obvious variability. We searched the light curves for features like eclipsing binaries, planetary transits and high amplitude pulsations.

Using the observations of each star, the mean value of magnitude and root mean square (r.m.s.) of the data were estimated. Figure 2(a) presents the standard deviation as a function of the instrumental magnitude in the V band. In this figure, stars with a large standard deviation are expected to be variables, while stars along the line having a smaller value of standard deviation are mostly non-variable comparison stars. Figure 2(b) shows right ascension (RA) and declination (Dec) (both in degrees) of 60 identified variables including the eight W UMa binaries in the field of M37. Figure 3(a), displays the M37 frame marked with all the selected stars used for ensemble photometry analysis and Figure 3(b) depicts 60 variable stars including W UMa stars using the tvmark task for the observed M37 field.

A star is considered as variable if its r.m.s. is greater than 3 times the mean r.m.s. The same criterion was adopted in Lata et al. (2012), Joshi et al. (2012), Wang et al. (2015) and Dutta et al. (2018).

3.1 Period Determination

We used (i) a Schuster periodogram and (ii) a Lomb-Scargle (LS) periodogram to obtain the most probable periods. Schuster (1897) demonstrated that a periodogram could yield information on periodic components of a time series and could be applied even when the periods are not known beforehand. The LS periodogram is used to determine the most probable period of a variable star (Lata et al. 2014) and has been developed to search for significant periodicities in unevenly sampled data (Scargle 1982; Horne & Baliunas 1986).

We used an LS periodogram to estimate the period of a star and the stars which have magnitude range $V < 20$ were considered for the variability search as photometric magnitudes have large errors towards the fainter end. After this, we visually inspected the light curves for periodic variation. Then, a phased light curve was derived for each star using an estimated period. In order to obtain the most probable periods for phase coverage, the LS periodogram appeared slightly better than the Schuster periodogram.

For some periodic variables, it was noticed that the period finding routine gives a best fit period that actually corresponds to half the orbital period. In order to detect such variables, we inspected the light phased at twice the period given by the period finding algorithms like LS and Schuster algorithms. In case of variables ID009, ID019, ID021, ID033, ID063, ID215, ID239 and ID250, the periods are indicated in the power spectrum (Figure 4) using the LS periodogram. By visual inspection we found that in eight cases the true period is twice the period obtained using the LS routine, because the light curves have two equal minima. In this way, we found eight W UMa binaries among 60 detected variables.

3.2 Astrometry

The (X, Y) pixel coordinates of variables found in M37 were converted into RA and Dec using IRAF ccmap and cctran tasks. ccmap computes the plate solution for an image using a list of matched pixels and celestial coordinates (40–50 stars from the VizieR 2MASS list) and sets up a mathematical translation called transformation between X and Y pixel coordinates in the image and RA and Dec coordinates. cctran applies the plate solution to a list of pixels or coordinates in the input and writes transformation coordinates for the whole frame. The accuracy of RA and Dec obtained using the above procedure is discussed in the following section.

4 COORDINATE MATCH

In order to match RA and Dec (in arcmin) of our observed objects with Messina et al. (2008) objects, celestial coordinates of 2641 objects from the VizieR list were chosen as reference. We plotted 2641 objects from the VizieR list represented by ▲, 122 objects from Messina et al. (2008) denoted by $*$ and our observed objects designated by □ as shown in Figure 5. After overplotting the three data sets, it was found that coordinates of our

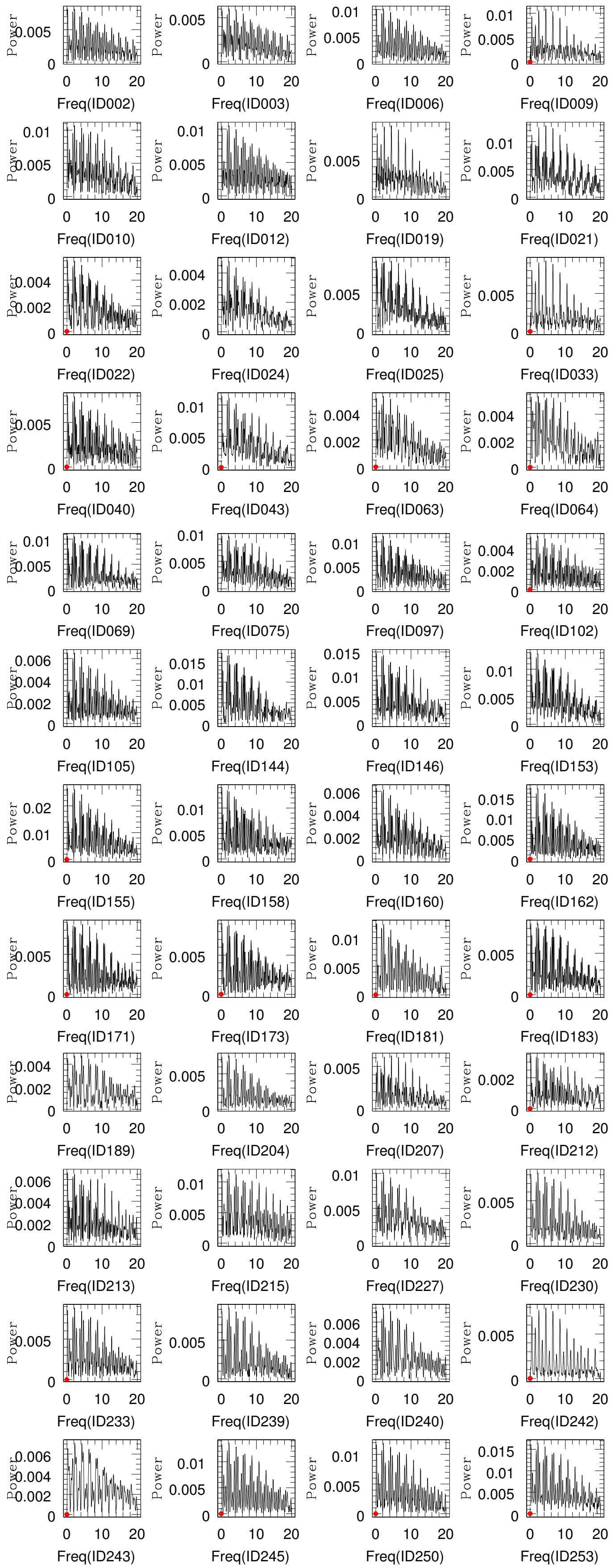

Fig. 4 Power spectrum using LS periodogram: power vs. frequency (in d^{-1}).

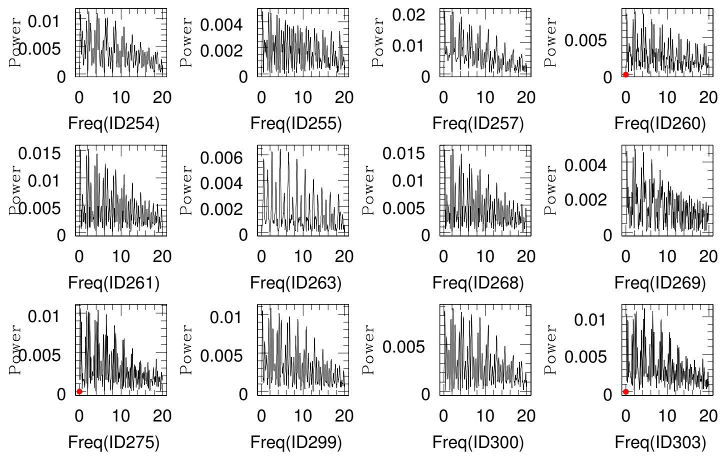

Fig. 4 — *Continued.*

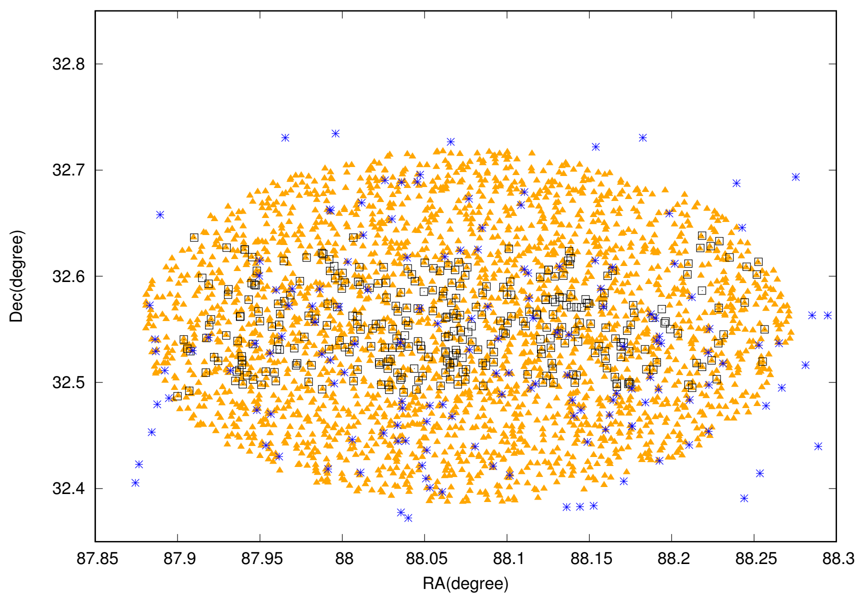

Fig. 5 α vs. δ in arcmin, VizieR coordinates (▲), Messina et al. (2008) coordinates ($*$) and our observed objects (□).

objects matched and fitted well with the VizieR list of objects, barring a few. We also noticed that Messina et al. (2008) coordinates are off from the values listed for VizieR objects. The above procedure lead to the identification of 60 new variable stars not reported earlier, among which eight are newly discovered W UMa binary systems. Table 2 lists α, δ, periods obtained using LS and Schuster periodograms, $\langle V \rangle$ and $\langle B - V \rangle$.

5 W UMA BINARY STARS IN M37

Eclipsing binaries exhibit specific features in observational data and are easily recognized. A part of the light is blocked as one component passes in front of the other, and the observed flux is diminished. This time dependent change in flux helps us to constrain the physical parameters of a binary system. An eclipse can be used to obtain the following information: (i) stellar masses, (ii) stellar radii, (iii) shape of eclipse indicating the inclination and (iv) surface brightness variations, i.e., gravity darkening, limb darkening, reflection, spots, etc.

W UMa binary systems can be recognized by their light curves with nearly equal minima. The periods of W UMa binaries are typically short, usually p <1 d (Luo et al. 2017; Rucinski 2006), $5 < p < 20$ h (Berdyugina 2005) or $0.2 < p < 0.8$ d (Kang et al. 2002). The

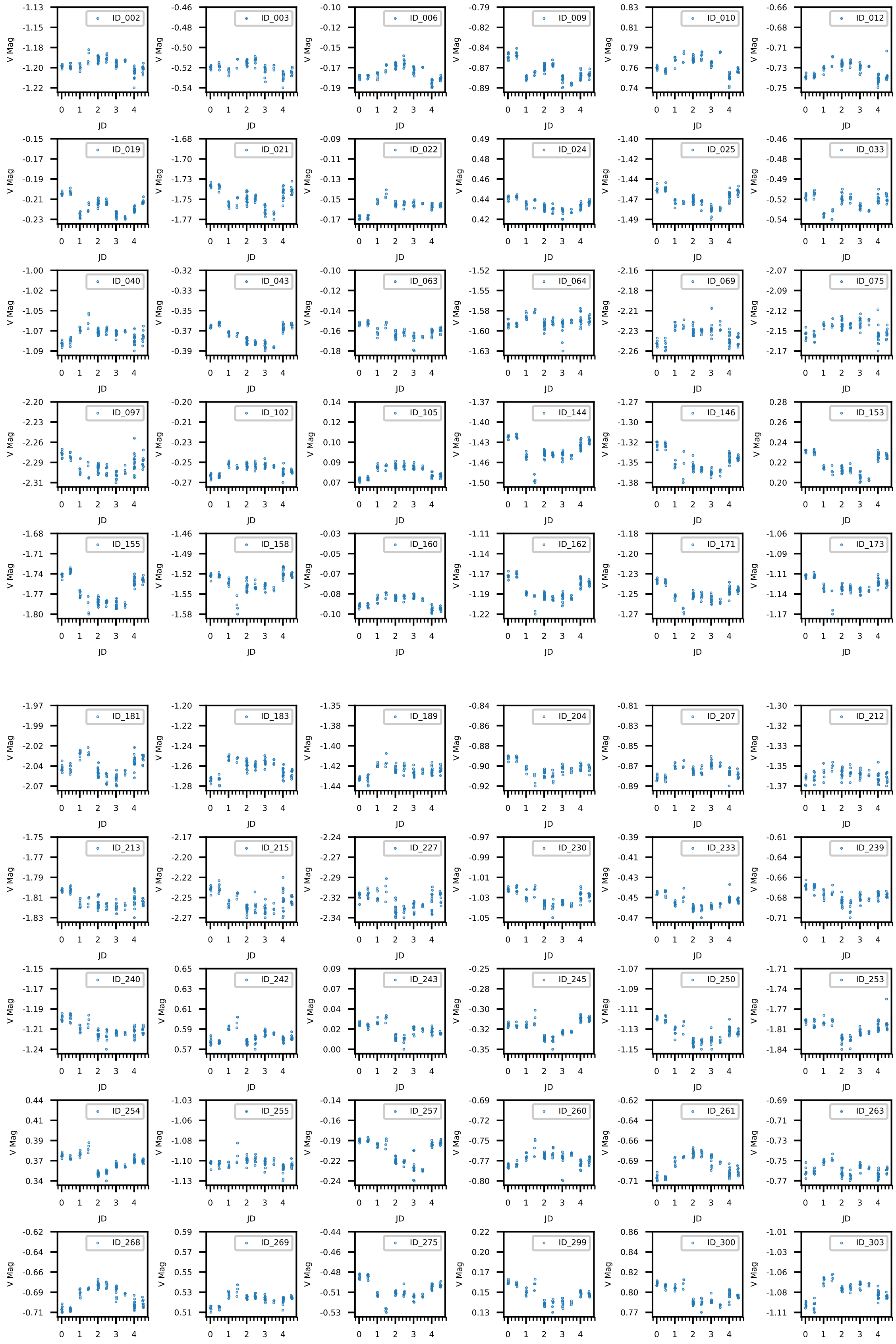

Fig. 6 JD(2457700+) vs. differential V magnitude of identified variables in M37.

Fig. 7 Phase plots of identified variables.

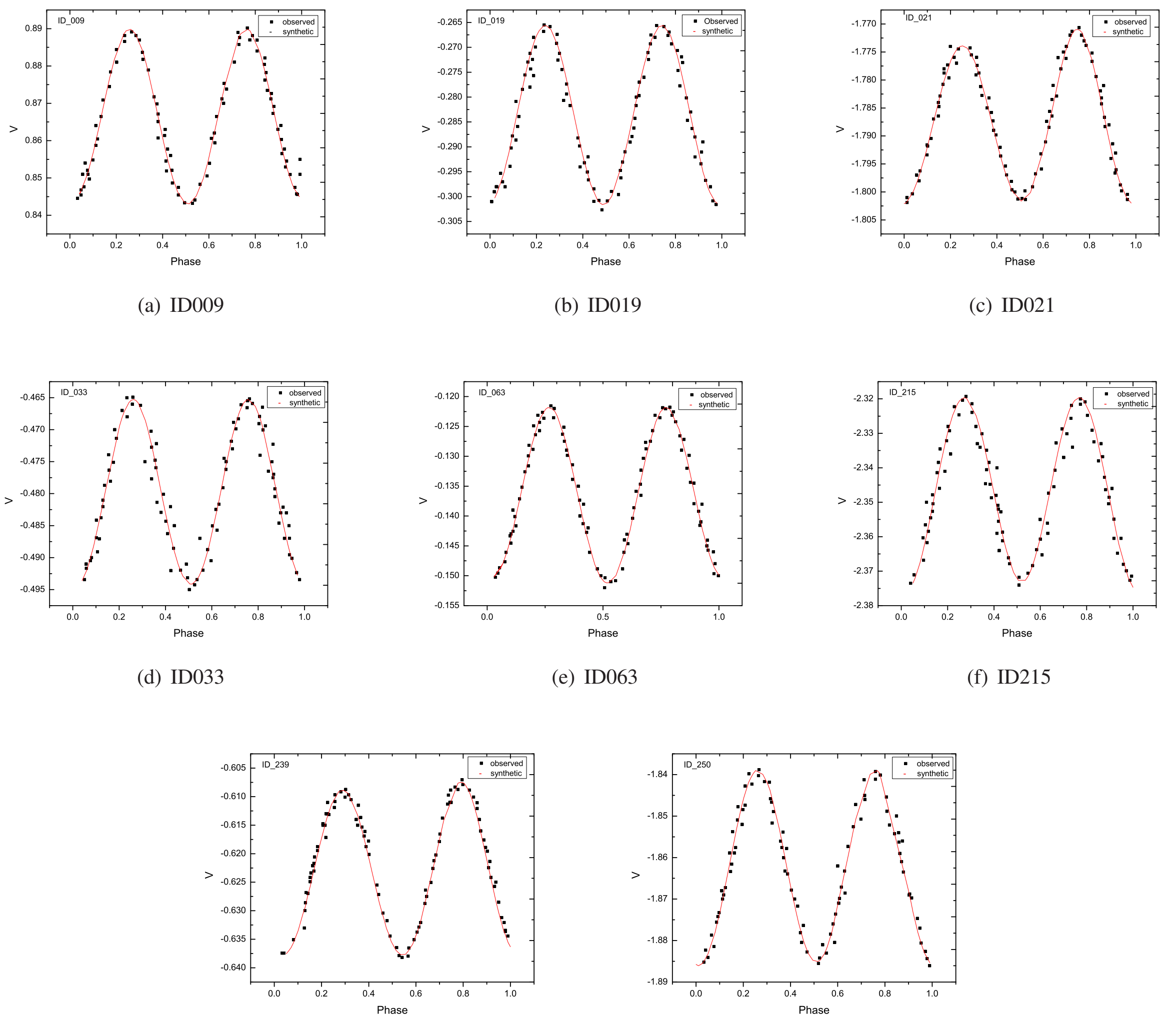

(a) ID009 (b) ID019 (c) ID021

(d) ID033 (e) ID063 (f) ID215

(g) ID239 (h) ID250

Fig. 8 W UMa binary stars in M37.

Table 3 A- and W-type W UMas

ID	q	W UMa type
ID009	0.78	A
ID019	0.91	A
ID021	1.42	W
ID033	1.09	W
ID063	0.75	A
ID215	1.32	W
ID239	1.05	W
ID250	5.52	W

components in W UMa systems are usually very close to each other, so that they overfill their critical Roche Lobe and share a common envelope (Luo et al. 2017). For this reason, they are called near or overcontact systems. One of the special characteristics of W UMa systems is that the effective temperatures of both components are very similar, although the masses are different. The presence of large star spots with strong chromospheric and coronal X-ray emissions was reported by Guinan & Bradstreet (1988), which signifies the presence of dynamo related magnetic activity. The first theoretical interpretation of W UMa binaries was proposed by Lucy (1967), who suggested that the two components of such a system share a common envelope with the same entropy, resulting in almost constant effective temperature over the surface of two stars (Paczyński et al. 2006). Kang et al. (2007) observed M37 and discovered nine δ Scuti type stars, seven eclipsing binaries and one pe-

Table 4 Photometric solutions of W UMa Binary Stars in M37

Parameter	ID009	ID019	ID021	ID033	ID063	ID215	ID239	ID250
i	51.8	61.9	122.5	53.9	47.4	22.2	61.9	63
Ω_1	3.290384	3.64838	4.722655	3.8418	3.261594	3.68675	4.137314	10.219298
Ω_2	2.941882	3.10031	3.83277	3.343726	2.904593	3.09867	3.283079	9.161445
$q = m_2/m_1$	0.78	0.91	1.42	1.09	0.75	1.32	1.05	5.52
$T_{\rm eff1}$ [K]	6320	6020	6220	6500	6320	5710	6220	6200
$T_{\rm eff2}$ [K]	6140	5920	6000	6000	6000	5350	6120	5800
R_1	1.422896	2.158887	2.292992	2.164679	2.7655	3.465474	1.925589	1.234882
R_2	1.222089	2.024612	2.824674	2.292705	2.309765	3.908218	1.965446	3.771656
$M_{2\rm bol}$	3.187434	2.937165	2.664363	2.34512	2.188241	2.202687	2.524282	3.195541
$M_{1\rm bol}$	3.491038	3.062941	2.2287	2.233496	2.553542	1.870123	2.469035	0.962055
$\log_{g1}$ 1	4.09662	4.477277	4.462321	4.379503	4.440356	3.991131	4.425912	4.569443
$\log_{g2}$ 2	4.120855	4.492095	4.433477	4.367021	4.471829	3.98184	4.429306	4.341569
Surf. Bright. 1	2.100853	0.11262	0.081116	0.103424	0.475476	1.267708	0.359898	1.153493
Surf. Bright. 2	2.144664	0.113733	0.078878	0.102787	0.486937	1.277068	0.358374	1.153493
PHSV	4.3	5.11503	5.9	5.1	4.4	4.1	5.4	13.69
PCSV	3.7	10	10	6.7	10	4	5.1	10
GRb1	0.32	0.32	0.32	0.32	0.32	0.32	0.32	0.32
GRb2	0.32	0.32	0.32	0.32	0.32	0.32	0.32	0.32
ALBEDO(ALB1)	0.6	0.6	0.6	0.6	0.6	0.6	0.6	0.6
ALBEDO(ALB2)	0.6	0.6	0.6	0.6	0.6	0.6	0.6	0.6

Notes: There is no evidence for spots on each binary star.

culiar variable. Among the seven eclipsing binaries, six stars were identified as W UMa type. Kiss et al. (2001) identified seven variable stars in the same open cluster using time series measurements. Among the identified variables, three were reported as W UMa type, two as long period eclipsing binaries and the remaining two as high amplitude δ Scuti type stars. Messina et al. (2008) observed this cluster and identified 122 periodic variables (out of which 16 were already known periodic variables) as cluster members. They also detected three detached eclipsing binaries. Based on their RA and Dec, we conclude that the W UMa binary systems we have identified are different from those reported earlier.

6 RESULTS AND CONCLUSIONS

In our observations of M37 during 2017, we discovered a total of 60 variables including eclipsing binaries as shown in Figures 6 and 7, where Figure 6 displays JD vs. differential magnitude and Figure 7 presents the phase plots of detected variables using the periods obtained from the LS routine. Among the 60 identified variables, eight are newly discovered eclipsing W UMa binary systems which are designated as ID009, ID019, ID021, ID033, ID063, ID215, ID239 and ID250. The photometric solutions of eight W UMa systems are obtained using PHysics Of Eclipsing BinariEs (PHOEBE), which is a synthetic light curve analysis technique based on the Wilson-Devinney (W-D) code (Wilson & Devinney 1971). PHOEBE estimates the physical parameters of eclipsing binaries that theoretically best match the data of user supplied experimental light curves and radial velocities (Prša & Zwitter 2005). The light curve analysis was carried out and photometric solutions were obtained for the eight identified W UMa binary stars in open cluster M37. The model fitted light curves of eight W UMa binaries are shown in Figure 8.

When utilizing PHOEBE for W UMa type overcontact binaries, we followed Lucy (1967) and applied the constraint that gravity darkening, bolometric albedo and limb darkening parameters of both the stars are the same. Gravity darkening coefficients for the components of the binaries were kept at 0.32 for convective envelopes and the bolometric albedos were taken as 0.6 for both components. Further, we set eccentricity e of the orbit as 0 for circular orbits in the case of convective and radiative atmospheres of contact binaries.

An important parameter to understand the evolution of a binary star is mass ratio. W UMa binaries have been categorized into two subclasses on the basis of observational characteristics: (i) A-type and (ii) W-type. A-type systems possess components typically from A to G spectral type having higher luminosity and lower mass ratio, i.e. $q = M_2/M_1 < 1$ (Binnendijk 1970). In case of an A-type W UMa, deeper minima are due to transit eclipses of a massive hot component. On the other hand, W-types are usually F to K spectral type and the deeper minima correspond to the occultation eclipse of the less massive smaller component with mass ratio $q = M_2/M_1 > 1$.

Table 3 lists the W- and A-type W UMa cases found in M37. The detected binaries have spectral types F, G and K as their $T_{\rm eff}$ ranges from 6500–4600 K.

The computed values of the angle of inclination for the detected binary systems vary from $22.2°$ for ID215 to $122.5°$ for ID021. The objects with inclination $i < 90°$ have counter clockwise rotation. The range for angle of inclination is shown in Table 4. The temperature difference ΔT between the components of binary system ID009 is 180 K, ID019 is 100 K, ID021 is 220 K, ID033 is 500 K, ID063 is 320 K, ID215 is 360 K, ID239 is 100 K and ID250 is 400 K. If the temperature difference between the components is around 1000 K or larger, they are classified as B-type W UMas and named poor thermal contact binaries by Rucinski & Duerbeck (1997). However, we did not detect any B-type W UMa binaries as the temperature difference between the components is less than 1000 K for all the detected W UMas in our survey.

The results obtained from the photometric analysis using PHOEBE of each binary system are provided in Table 4. This is the first photometric study of these newly identified W UMa systems and the solutions may not give all the physical properties of these systems precisely. Moreover, M37 was observed earlier by other authors as already discussed in this paper. It is important to have future long term photometric and possibly spectroscopic observations of the M37 open cluster to discover new variables, in general, and W UMa binary stars, in particular.

Acknowledgements One of the authors, Ajaz Ahmad Dar, is thankful to the University Grants commission, New Delhi for awarding the Faculty Development Programme (teacher fellowship for pursuing Ph.D.) and Islamia College of Science and Commerce, Srinagar for deputation to the University of Kashmir for the said programme. Ajaz Ahmad Dar is thankful to the Director of the Indian Institute of Astrophysics (IIA), Bangalore for hosting him at IIA for extended periods.

References

Berdyugina, S. V. 2005, Living Reviews in Solar Physics, 2, 8
Binnendijk, L. 1970, Vistas in Astronomy, 12, 217
Dar, A. A., Parihar, P. S., Saleh, P., & Malik, M. A. 2018a, New Astron., 64, 34
Dar, A. A., Parihar, P. S., & Malik, M. A. 2018b, RAA (Research in Astronomy and Astrophysics), 18, 112
Dutta, S., Mondal, S., Joshi, S., et al. 2018, MNRAS, 476, 2813
Gilliland, R. L., & Brown, T. M. 1988, PASP, 100, 754
Guinan, E. F., & Bradstreet, D. H. 1988, in NATO Advanced Science Institutes (ASI) Series C, 241, eds. A. K. Dupree & M. T. V. T. Lago, 345
Hargis, J. R., Sandquist, E. L., & Bradstreet, D. H. 2005, AJ, 130, 2824
Hartman, J. D., Gaudi, B. S., Holman, M. J., et al. 2008, ApJ, 675, 1254
Horne, J. H., & Baliunas, S. L. 1986, ApJ, 302, 757
Joshi, Y. C., Joshi, S., Kumar, B., Mondal, S., & Balona, L. A. 2012, MNRAS, 419, 2379
Kang, Y. B., Kim, S.-L., Rey, S.-C., et al. 2007, PASP, 119, 239
Kang, Y. W., Oh, K.-D., Kim, C.-H., et al. 2002, MNRAS, 331, 707
Kiss, L. L., Szabó, G. M., Sziládi, K., et al. 2001, A&A, 376, 561
Lata, S., Pandey, A. K., Maheswar, G., Mondal, S., & Kumar, B. 2011, MNRAS, 418, 1346
Lata, S., Pandey, A. K., Chen, W. P., Maheswar, G., & Chauhan, N. 2012, MNRAS, 427, 1449
Lata, S., Yadav, R. K., Pandey, A. K., et al. 2014, MNRAS, 442, 273
Lucy, L. B. 1967, ZAp, 65, 89
Luo, C., Zhang, X., Deng, L., et al. 2017, New Astron., 52, 29
Messina, S., Distefano, E., Parihar, P., et al. 2008, A&A, 483, 253
Paczyński, B., Szczygieł, D. M., Pilecki, B., & Pojmański, G. 2006, MNRAS, 368, 1311
Parihar, P., Messina, S., Distefano, E., Shantikumar, N. S., & Medhi, B. J. 2009, MNRAS, 400, 603
Prša, A., & Zwitter, T. 2005, ApJ, 628, 426
Rucinski, S. M. 2006, MNRAS, 368, 1319
Rucinski, S. M., & Duerbeck, H. W. 1997, PASP, 109, 1340
Scargle, J. D. 1982, ApJ, 263, 835
Schuster, A. 1897, Proceedings of the Royal Society of London Series I, 61, 455
Stetson, P. B. 1987, PASP, 99, 191
Wang, K., Deng, L., Zhang, X., et al. 2015, AJ, 150, 161
Wilson, R. E., & Devinney, E. J. 1971, ApJ, 166, 605